Journal of Nuclear Materials 392 (2009) 353–359

Contents lists available at ScienceDirect

Journal of Nuclear Materials

journal homepage: www.elsevier.com/locate/jnucmat

Mechanical properties of irradiated ODS-EUROFER and nanocluster strengthened 14YWT

D.A. McClintock [a,b,*], M.A. Sokolov [b], D.T. Hoelzer [b], R.K. Nanstad [b]

[a] University of Texas at Austin, Austin, TX 78712, USA
[b] Materials Science and Technology Division, Oak Ridge National Laboratory, Oak Ridge, TN 37831-6151, USA

A B S T R A C T

Irradiations to 1.5 dpa at 300–750 °C were conducted to investigate the changes in mechanical properties of an advanced nanocluster strengthened ferritic alloy, designated 14YWT, and an oxide dispersion strengthened ferritic alloy ODS-EUROFER. Two non-dispersion strengthened variants, 14WT and EUROFER 97, were also irradiated and tested. Tensile results show 14YWT has very high tensile strengths and experienced some radiation-induced hardening, with an increase in room temperature yield strength of 125 MPa after irradiation, while results for ODS-EUROFER show a 275 MPa increase following irradiation. Master curve fracture toughness analysis show 14YWT has a cryogenic T_o reference temperatures before and after irradiation of about −188 and −176 °C, respectively, and upper-shelf $K_{J_{ic}}$ values between 175 and 225 MPa$\sqrt{m}$. The favorable fracture toughness properties and resistance to radiation-induced changes in mechanical properties observed for 14YWT are attributed to a fine grain structure and high number density of Y–Ti–O nanoclusters.

1. Introduction

Oxide dispersion strengthened (ODS) ferritic alloys containing a high number density of small oxide particles have been investigated for use as fuel cladding and structural applications in nuclear systems for several decades, not only because of they have excellent high-temperature tensile properties and creep resistance, but because the particles also increase an alloy's resistance to radiation-induced changes in mechanical properties and swelling [1,2]. Recent research efforts in Europe to produce an optimized reference ferritic alloy for high-temperature structural applications in nuclear environments have been focused on a 9CrW reduced activation ferritic/martensitic (RAFM) steel, designated EUROFER 97 [3]. ODS variants of EUROFER 97 were developed to increase the service temperature from 550 to 650 °C by improving high-temperature strength and creep resistance. ODS-EUROFER was produced by mechanical alloying small amounts (0.2–0.3 wt%) of Y_2O_3 powder with gas atomized EUROFER 97 powder followed by consolidation using hot isostatic pressing. Though tensile and creep properties of ODS-EUROFER were impressive, early results showed oxide dispersion strengthening reduced impact toughness and produced a relatively high ductile to brittle transition temperature (DBTT) compared to non-ODS conventional ferritic alloys [4,5]. Subsequent studies attributed the reduced impact toughness and ductility of ODS-EUROFER to the formation of $M_{23}C_6$ type precipitates along grain boundaries [6,7]. Recent optimization of ODS-EUROFER processing and heat treatment to promote dissolution of the large $M_{23}C_6$ precipitates has produced an alloy with improved impact toughness and tensile ductility compared to the initial alloy variants [7].

The recent discovery of nanoclusters in mechanically alloyed ferritic alloys using three-dimensional atom probe tomography (3D-APT) has opened a new area of study of dispersion strengthened materials and generated much interest in the materials community concerning the resistance to radiation-induced changes in mechanical properties for this class of material [8]. 3D-APT examinations have shown advanced nanostructured ferritic alloys (NFAs) contain a high number density (1.4×10^{24} m^{-3}) of ultra-fine (2–5 nm) regions enriched in Y, Ti, and O atoms, called nanoclusters (NC), uniformly distributed in the ferritic lattice [9]. High-temperature annealing studies using local electrode atom probe (LEAP) has shown nanoclusters are remarkably stable at high temperatures and do not appreciably coarsen or decrease in number density after isothermal aging at 1300 °C for 24 h [10]. The small size and high number density of nanoclusters in NFAs are responsible for their superior tensile strengths and creep resistance compared to conventional ODS ferritic alloys [11]. This high number density of nanoclusters may also provide effective trapping centers for point defects and transmutation products produced during neutron irradiation, possibly mitigating their effect on bulk material properties [12,13].

* Corresponding author. Address: Materials Science and Technology Division, Oak Ridge National Laboratory, Oak Ridge, TN 37831-6151, USA. Tel.: +1 865 241 2955; fax: +1 865 241 3650.
E-mail address: mcclintockda@ornl.gov (D.A. McClintock).

0022-3115/$ - see front matter © 2009 Elsevier B.V. All rights reserved.
doi:10.1016/j.jnucmat.2009.03.024

Though NFAs were shown to have impressive tensile strengths compared to other RAFM steels, fracture toughness results from an early NFA alloy, designated 12YWT, revealed poor fracture toughness properties. Initial fracture toughness test results indicated 12YWT has a fracture toughness transition temperature near 75 °C, a T_o master curve reference temperature of 102 °C, and a ductile initiation upper-shelf fracture toughness value, $K_{J_{Ic}}$, of about 93 MPa$\sqrt{m}$ at 100 °C [14]. Ferritic alloys undergo a transition from ductile deformation behavior at high temperatures to brittle fracture behavior at low temperatures; the narrow temperature range over which this transition occurs is called the fracture toughness transition temperature (FTTT). The FTTT reported in this paper is the midpoint temperature in the transition region between complete brittle fracture and complete ductile tearing behavior. Following these disappointing results another NFA was produced using modified production and processing parameters, as well as sight composition changes, in an effort to improve grain structure and fracture toughness properties. The new alloy, designated 14YWT, was produced by mechanically alloying a 14 wt% Cr (2% more than 12YWT) ferritic steel base powder with 0.3 wt% Y_2O_3 powder (compared to 0.25 wt% for 12YWT) followed by extrusion at 850 °C (decreased from 1150 °C for 12YWT). Transmission electron microscopy (TEM) examination revealed that 14YWT has a more refined microstructure with a lower aspect ratio (1–5) and sub-micrometer grain size compared to the first generation NFA 12YWT, which has an aspect ratio of ~10 with grains roughly 5–20 μm in length and 1 μm width, seen in Fig. 1 [15]. The initial fracture toughness results showed 14YWT had a very low FTTT of about −150 °C and improved upper-shelf $K_{J_{Ic}}$ values around 175 MPa$\sqrt{m}$ [15].

This paper summarizes unirradiated and irradiated tensile and fracture toughness properties of a recent experimental extrusion of 14YWT, which is currently being developed at Oak Ridge National Laboratory (ORNL), and an optimized European ODS ferritic alloy ODS-EUROFER. To quantify the contribution of dispersion strengthening for each alloy, non-dispersion strengthened variants of each alloy were also tested in the unirradiated and irradiated condition. An alloy, designated 14WT, was produced using the identical ferritic base powder and processing/extrusion parameters used for 14YWT, but without the Y_2O_3 powder addition prior to ball milling. Previous work has shown that an addition of Y_2O_3 powder during ball milling is required for nanocluster formation during powder consolidation [16]. Specimens of a non-ODS-EUROFER 97 ferritic/martensitic alloy were also produced and tested in the unirradiated and irradiated condition. Tensile and fracture toughness test were performed on all materials to quantify the effect of irradiation on mechanical properties.

2. Experimental procedure

The experimental ODS-EUROFER alloy was provided by Rainer Lindau (Forschungszentrum Karlsruhe, Germany) in a final processed plate form. The plate was produced by Plansee, with parameters defined by Lindau, using an industrial attritor type ball mill for mechanical alloying and hot isostatic pressing for powder consolidation. The consolidated alloy was hot rolled at 1150 °C, air-cooled to room temperature, normalized in an argon atmosphere at 1100 °C for 30 min, and water quenched to produced an ODS ferritic alloy with a ferritic/martensitic microstructure; this alloy contained a relatively low carbon content (~0.08 wt%) and water-cooling was required to induce martensite formation. The plate was then tempered in an argon atmosphere at 750 °C for 2 h and air-cooled. To serve as a comparison material for this heat of ODS-EUROFER, specimens were also produced from conventional non-ODS-EUROFER 97 and tested in the unirradiated and irradiated condition. Similar to 14WT and 14YWT, EUROFER 97 served as a model alloy for ODS-EUROFER without oxide dispersions and allowed quantification of the effect of oxide particles on mechanical properties and radiation resistance.

The 14YWT and 14WT alloys were produced at ORNL using high-energy mechanical alloying and warm extrusion. 14WT was produced using identical parameters used for 14YWT, but without the 0.3 wt% Y_2O_3 powder addition required for NC formation. The Fe–14Cr–3W–0.4Ti (nominal wt%) ferritic base powder for 14YWT and 14WT production was supplied by Special Metals (Princeton, KY, USA) and sieved with ASTM sizes +325 to −100 to produce a particle size distribution of 45–150 μm. The Y_2O_3 powder was supplied by Nanophase Technologies Corporation (Romeoville, IL, USA) with a particle size distribution of 17–31 nm. The ferritic base powder for 14YWT was mechanically alloyed with the Y_2O_3 powder using a Simoloyer CM01 high-energy horizontal attritor type ball mill produced by Zoz GmbH (Wenden, Germany); the base ferritic powder used to produce 14WT was ball milled without Y_2O_3 using the same parameters as used for 14YWT. Four 200 g batches of 14YWT and 14WT powders were milled for 40 h in an inert argon atmosphere to produce 800 g of powder for each extrusion. After mechanical alloying the powders were degassed and sealed in extrusion cans designed for a 7:1 reduction-in-area, which were preheated to 850 °C for 1 h before extrusion. The extruded bars

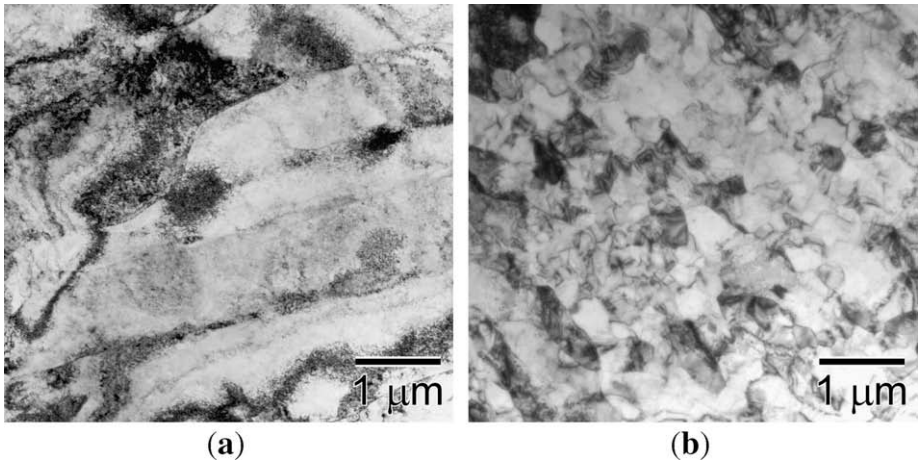

Fig. 1. Bright-field TEM images of (a) 12YWT and (b) 14YWT microstructures, reproduced from McClintock et al. [15].

were cut into 51 mm sections and machined by wire electric discharge machining (EDM) along the top and bottom length of each bar to create flat surfaces for rolling. The bars were then annealed at 1000 °C for 1 h in an air furnace and air-cooled. Each bar was preheated to 850 °C for 1 h and rolled in the extrusion direction using multiple passes (~5% per pass) to produce a total reduction-in-thickness of 40%.

For this study miniaturized tensile specimens and dual-notch three-point bend bars were irradiated in small 'rabbit' capsules in the High Flux Isotope Reactor (HFIR) at ORNL. The tensile specimen was a small sheet-type tensile specimen (gauge section dimensions: 7.62 × 1.52 × 0.76 mm) that was tested by loading the shoulders of the specimen heads near the gauge section using a custom specimen holder. The fracture toughness specimen utilized was a dual-notch three-point bend bar, allowing two tests per bar; dimensions are detailed elsewhere [15]. Tensile and fracture toughness specimens were machined from the rolled 14WT and 14YWT bars and the final processed EUROFER 97 and ODS-EUROFER plates using wire EDM. The tensile specimens were machined in the L orientation, while the bend bars were machined in the L-T orientation as specified in ASTM E 399–06 for extruded or rolled plate material.

Specimens were irradiated to a nominal fluence of 2.1×10^{21} n/cm^2 [$E > 0.1$ MeV], corresponding to 1.5 displacements per atom (dpa), in 'rabbit' capsules located in the HFIR center flux trap target positions. 'Rabbit' capsules are small tubes made of aluminum (6061–T6) and vanadium (V–4Cr4Ti) alloys that contain mechanical and/or microstructural characterization specimens sealed inside. These sealed capsules were designed to maintain irradiation temperatures of 300, 600, and 750 °C for tensile specimens and 300 °C for the bend bars. Results from later examination of SiC temperature monitors included in the capsules during irradiation revealed the actual irradiation temperatures for the 600 and 700 °C tensile specimen capsules were 580 and 670 ± 20 °C, respectively. Extensive prior experience with the 300 °C irradiation temperature capsule design has repeatedly shown an actual irradiation temperature of 300 ± 20 °C [17], therefore SiC monitors were not measured for these capsules.

Unirradiated tensile specimens were tested from −196 to 700 °C for most of the alloys and irradiated specimens were tested from room temperature to the irradiation temperature; all tensile tests were performed at a strain rate of 10^{-3} s^{-1}. Fracture toughness bend bars were fatigue precracked prior to testing to produce an initial crack length to specimen width (a_o/W) ratio of 0.5; the precise initial crack length was measured from the fracture surface of each specimen after testing and used during data analysis for J_c and J_{Ic} calculations. Fracture toughness tests were performed in a three-point bend configuration using the unloading compliance method; fracture toughness testing procedures were closely scrutinized to ensure ASTM E 1820–06 validity requirements were met. The fracture toughness stress intensity factors for brittle cleavage failure behavior,K_{J_c}, were calculated from the critical J-integral values at fracture, J_c, and then size adjusted to results for a 1-T reference specimen, $K_{J_c(1T)}$, as specified in ASTM E 1921–05. The size adjustment of fracture toughness values in the ductile to brittle transition region to those for a 1-T reference specimen is used to compensate for effects caused by a relatively small fracture toughness specimen and allow for comparative analysis with other ferritic alloys tested in the transition region. The size adjusted $K_{J_c(1T)}$ values were then used to calculate a master curve reference temperature, T_o, for each material in the unirradiated and irradiated condition to quantify any radiation-induced shift in FTTT. In the fully ductile region stress intensity factors, $K_{J_{Ic}}$, were calculated for specimens experiencing stable crack growth using the critical J-integral values at the onset of stable crack growth, J_{Ic}, which were determined from J–R curves as defined in ASTM E 1820–06.

3. Results and discussion

All tensile test results are summarized in Table 1. Unirradiated tensile results for 14YWT and ODS-EUROFER show a clear distinc-

Table 1
Tensile results for alloys tested in unirradiated and irradiated conditions. All irradiated specimens exposed to a nominal 1.5 dpa at the indicated temperatures.

Material (Condition)	Test temperature (°C)	Yield strength (MPa)	UTS (MPa)	Failure strength (MPa)	Uniform elongation (%)	Total elongation (%)
EUROFER 97	26	555	682	393	6.4	19.7
(unirradiated)	300	511	559	313	3.2	13.5
EUROFER 97	25	792	793	435	0.3	10.8
(T_{irr} = 300 °C)	300	729	730	393	0.2	8.7
ODS EUROFER	26	966	1085	725	3.8	11.7
(unirradiated)	300	911	969	685	2.4	9.2
ODS EUROFER	25	1243	1254	811	0.4	7.1
(T_{irr} = 300 °C)	300	1142	1145	749	0.3	6.8
14WT	26	743	935	608	11.0	21.3
(unirradiated)	300	601	726	496	6.4	13.5
14WT	20	999	1059	736	9.6	18.6
(T_{irr} = 300 °C)	300	824	949	640	9.6	18.6
14WT	24	651	881	620	10.0	18.9
(T_{irr} = 580 °C)	580	474	535	328	3.4	12.7
14WT	24	727	924	657	9.9	18.9
(T_{irr} = 670 °C)	670	352	373	39	1.1	17.0
14YWT	26	1435	1564	1166	0.8	12.0
(Unirradiated)	300	1326	1384	1004	0.7	8.0
14YWT	20	1560	1641	1219	0.6	7.4
(T_{irr} = 300 °C)	300	1356	1430	1063	0.6	8.3
14YWT	24	1468	1653	1293	1.0	7.3
(T_{irr} = 580 °C)	580	937	1040	799	1.1	8.5
14YWT	24	1443	1466	1198	0.6	7.5
(T_{irr} = 670 °C)	670	627	693	505	1.2	11.0

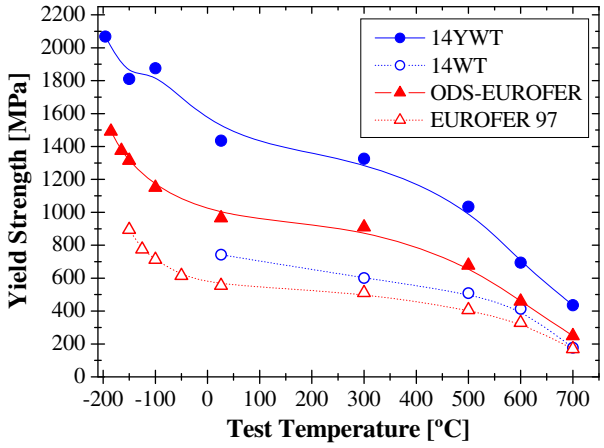

Fig. 2. Yield strength versus test temperature – unirradiated alloys.

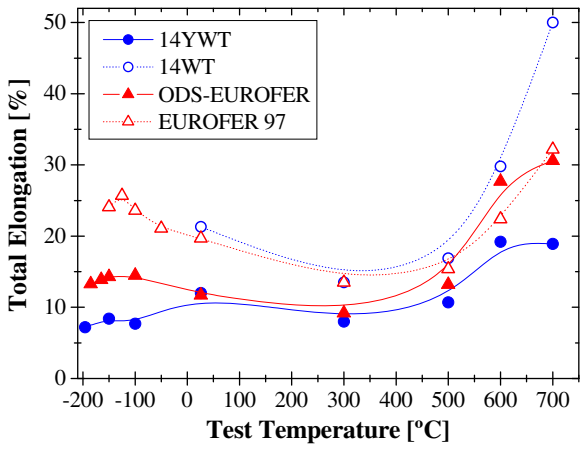

Fig. 3. Total elongation versus temperature – unirradiated alloys.

tion in the magnitude of strengthening between these dispersion strengthened ferritic alloys; with ~1450 MPa measured for yield strength of 14YWT at room temperature, while ODS-EUROFER yielded at ~960 MPa. The excellent high-temperature tensile strength of the two alloys is seen in Fig. 2, where at 600 °C 14YWT and ODS-EUROFER have measured yield strengths of 690 and 460 MPa, respectively. The large yield strength observed for 14WT, 740 MPa at 26 °C, is attributed to the Ti-rich oxide dispersions formed in the microstructure during mechanical alloying and extrusion. Although no Y_2O_3 was included during mechanical alloying of 14WT, the 0.4 wt% Ti in the base ferritic alloy cause 10–50 nm Ti-rich oxide particles to precipitate throughout the microstructure during extrusion [18]. Elongation data for ODS-EUROFER and 14YWT show very similar total elongation behavior, seen in Fig. 3, with room temperature total elongation of both alloys around 10–12%. However, uniform elongation was quite different; as shown in Fig. 4 the room temperature uniform elongation of ODS-EUROFER (~3.5%) was more than three times the value observed for 14YWT (~1.0%). The uniform elongation for 14WT was larger than EUROFER 97 for all temperatures below 700 °C, where the values for the two alloys converge to about 3%. Uniform elongation values for 14YWT and ODS-EUROFER remain lower than those of the two non-dispersion strengthened alloys for temperatures below 500 °C, where the values for 14WT and EUROFER 97 decrease rapidly while the values for 14YWT and ODS-EUROFER increase to 4.6 and 6.8%, respectively, at 700 °C.

The tensile test results for irradiated 14YWT and 14WT, shown in Fig. 5, show yield strength of each alloy responded differently to neutron irradiation. No considerable change in yield strength was

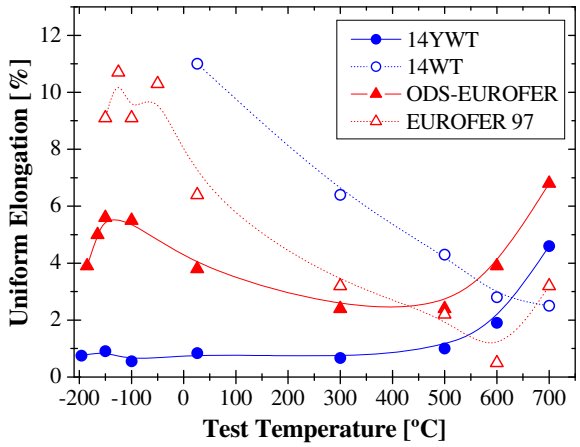

Fig. 4. Uniform elongation versus test temperature – unirradiated alloys.

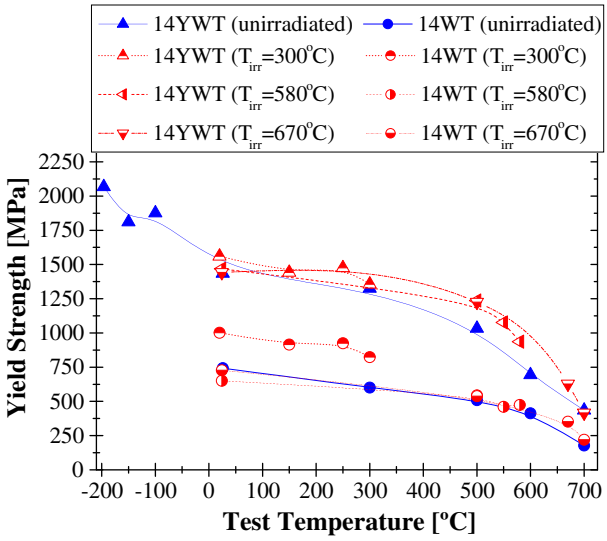

Fig. 5. Yield strength of 14YWT and 14WT – irradiated to 1.5 dpa at 300, 580, and 670 °C.

observed for 14WT irradiated at 580 and 670 °C, but a significant increase of about ~250 MPa was recorded at all test temperatures for specimens irradiated at 300 °C. Some hardening was observed for 14YWT specimens irradiated at 300 °C, with an increase in yield strength of about a 125 MPa (~9% increase) at room temperature, while an increase ranging from 10 to 215 MPa (~1–20% increase) was observed for most specimens irradiated at 580 and 670 °C. The tensile results for the two EUROFER alloys irradiated at 300 °C, seen in Fig. 6, showed uniform hardening for all test temperatures; an increase in yield strength of 225–275 MPa (~19–29% increase) was measured for ODS-EUROFER, while an increase of 185–225 MPa (~36–41% increase) was observed for EUROFER 97. The total elongation for irradiated 14YWT and 14WT, seen in Fig. 7, shows little loss of ductility for either alloy up to about 500 °C, with some irradiated 14WT specimens tested at intermediate test temperatures (~100–300 °C) actually exhibiting larger total elongations than unirradiated specimens. Above ~500 °C both alloys show some loss of ductility for specimens irradiated at 670 °C, though more embrittlement was observed for 14WT; at 700 °C the total elongation of 14WT and 14YWT decreased by about 25% and 6%, respectively. The elongation data for irradiated EUROFER 97 and ODS-EUROFER in Fig. 8 show both alloys experienced a loss of ductility following irradiation at 300 °C; total elongation measured for EUROFER 97 decreased about 6–9%, while ODS-EUROFER decreased about 5% for all test temperatures.

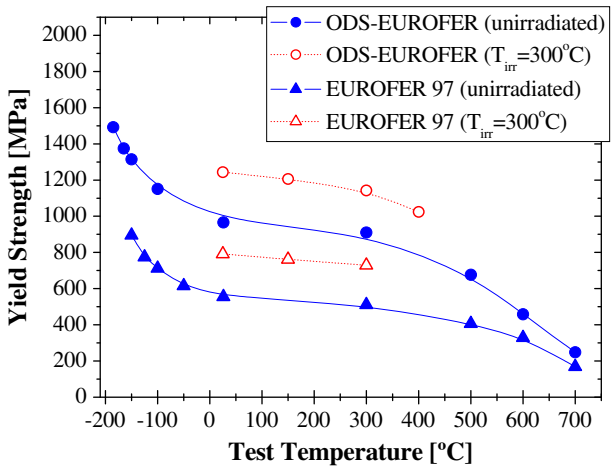

Fig. 6. Yield strength of EUROFER 97 and ODS-EUROFER – irradiated to 1.5 dpa at 300 °C.

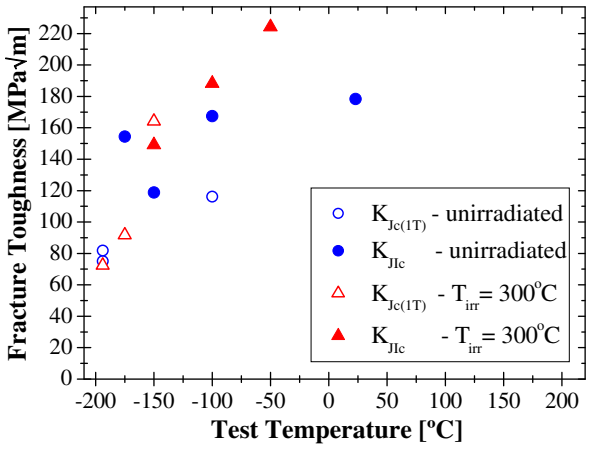

Fig. 9. Fracture toughness stress intensity values of 14YWT – irradiated and unirradiated.

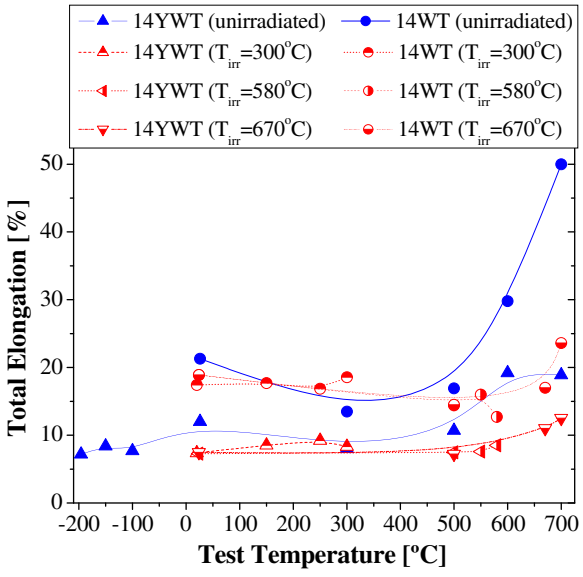

Fig. 7. Total elongation of 14YWT and 14WT – irradiated to 1.5 dpa at 300, 580, and 670 °C.

The fracture toughness results in Fig. 9 show that the transition from ductile to brittle fracture behavior for 14YWT occurs at very low temperatures; stable crack growth was observed in both an unirradiated specimen tested at −175 °C and an irradiated specimen tested at −150 °C. The unirradiated and irradiated data fall on top of one another, and the irradiated upper-shelf result at −50 °C appears to be larger than the upper-shelf results from unirradiated specimens. In the fully ductile region the stress intensity converted from the *J*-integral at the onset of stable crack growth, $K_{J_{Ic}}$, for 14YWT in the unirradiated and irradiated condition were about 175 and 225 MPa$\sqrt{}$m, respectively. Exposure to 1.5 dpa at 300 °C appears to have little effect on the transition temperature but may have increased the upper-shelf values in the fully ductile region, although these results from the small number of specimens need to be verified with a larger sample set. The fracture toughness results in Fig. 10 show ODS-EUROFER also has a low temperature ductile to brittle transition, with stable crack growth observed in an unirradiated specimen tested at −100 °C and an irradiated specimen tested at −90 °C.

Master curve analysis of the fracture toughness data for each alloy was performed to calculate the master curve reference temperature, T_o, which is used to characterize the ductile to brittle transition region and allow objective, quantitative comparison of transition behavior between different alloys. The T_o reference temperatures for the four alloys are given in Table 2 for the unirradi-

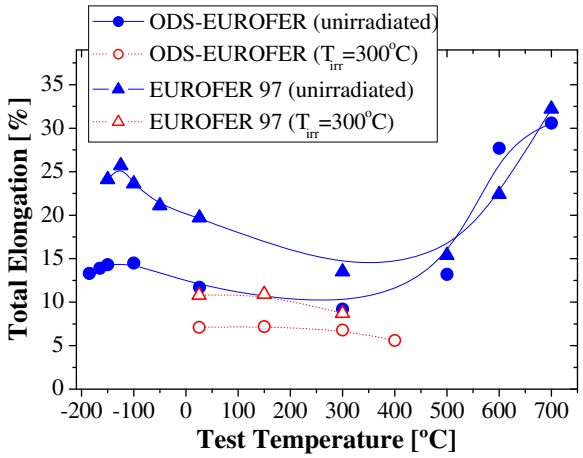

Fig. 8. Total elongation of EUROFER 97 and ODS-EUROFER – irradiated to 1.5 dpa at 300 °C.

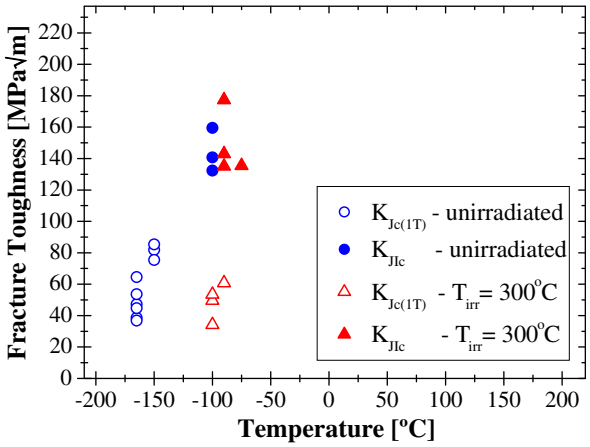

Fig. 10. Fracture toughness stress intensity values for ODS-EUROFER – irradiated and unirradiated.

Table 2
Master curve T_o reference temperatures – unirradiated and irradiated.

Alloy	T_o – unirradiated (°C)	T_o – irradiated (°C)	ΔT_o (°C)
14WYT	−188	−176	12
14WT	−112	−31	81
EUROFER 97	−120	−81	39
ODS-EUROFER	−115	−30	85

ated and irradiated condition. The extruded alloys 14YWT and 14WT had T_o reference temperatures of −188 and −112 °C, respectively. The two EUROFER alloys also had relatively low T_o temperatures, with −120 and −115 °C calculated for EUROFER 97 and ODS-EUROFER, respectively, which his comparable to the T_o value of about −105 °C for the conventional RAFM steel F82H [14]. All alloys experienced some increase in T_o reference temperature following irradiation, but 14YWT had the smallest shift; with only a 12 °C increase in T_o following irradiation. EUROFER 97 exhibited a moderate shift in T_o of about 39 °C, while the increase measured for 14WT and ODS-EUROFER was more pronounced at 81 and 85 °C, respectively.

The fracture toughness results for 14YWT in the unirradiated condition show a T_o value of −188 °C, an upper-shelf $K_{J_{Ic}}$ value of approximately 175 MPa$\sqrt{m}$, while after irradiation the $K_{J_{Ic}}$ values were 190 and 225 MPa$\sqrt{m}$ with only a 12 °C increase in T_o. These favorable fracture toughness results for 14YWT are similar to another nanocluster strengthened ferritic alloy designated MA957, which was developed and commercially produced by the International Nickel Company (INCO) [19]. MA957 and 14YWT are very similar: both alloys are produced through mechanical alloying and extrusion, have similar nominal compositions: Fe–14 wt%Cr–0.9Ti–0.3Mo–0.25Y_2O_3 and Fe–14 wt%Cr–3W–0.4Ti–0.3Y_2O_3, respectively, and both have been shown to contain a fine dispersion of small 2–10 nm Y–Ti–O enriched nanoclusters [9,20]. Previous work with MA957 has shown the upper-shelf $K_{J_{Ic}}$ values to be about 130 MPa$\sqrt{m}$ and a FTTT between −80 and −100 °C when tested in C-R orientation [21]. The low toughness values observed for MA957 were attributed to alumina stringers embedded in the microstructure during extrusion, and it was predicted that an alloy similar to MA957 with fewer stringers and reduced grain anisotropy would have improved fracture toughness. The grain structure of 14YWT has relatively fewer stringers, a sub-micrometer grain size (∼100 nm–1 μm), and a lower aspect ratio (∼1–5) compared to MA957 (∼10). The preliminary results outline here show that indeed 14YWT has improved fracture toughness properties with increased upper-shelf $K_{J_{Ic}}$ values near 225 MPa$\sqrt{m}$ and a lower FTTT of about −175 °C, compared to an upper-shelf $K_{J_{Ic}}$ value around 130 MPa$\sqrt{m}$ and a FTTT of about −80 °C for MA957 [21].

In addition to an improved grain structure, 14YWT has a very high number density ($\sim 2 \times 10^{24}$ m^{-3}) of nanoclusters that are thought to have a coherent interface with the surrounding ferritic matrix. Conventional oxide particles in ODS materials generally do not have fully coherent interfaces with the surrounding lattice, whereas recent work has suggested that nanoclusters in 14YWT are Y, Ti, and O atoms positioned on a continuation of the body centered cubic crystal structure that may be stabilized by O-vacancy pairs produced during mechanical alloying [22]. The large oxide particles found in conventional ODS alloys may generate relatively large microcracks at the particle/matrix interface, which produce higher stress concentration at the tips of those microcracks and may result in premature propagation of cracks. The coherent structure of Y–Ti–O nanoclusters may significantly reduce the number and size of microcracks at the nanocluster/matrix interface, which may increase the stress and time required to cause microcracks to reach critical size for propagation compared to conventional ODS ferritic alloys. Though nanoclusters appear to increase the fracture toughness of ferritic alloys and increase resistance to radiation-induced changes, more research is needed to fully understand the interactions taking place between nanoclusters and microcrack defects.

These results suggest the nanocluster strengthened alloy 14YWT has favorable fracture toughness and is more resistant to radiation-induced shift in FTTT compared to conventional ODS ferritic alloys. The 14WT and EUROFER 97 specimens tested in the fully ductile upper-shelf region did not experienced stable crack growth, only crack tip blunting, and the results from these tests were not included in the T_o reference temperature calculations for these two alloys. Crack blunting during testing in the upper-shelf region indicate the specimen size being used is not large enough for the particular material being examined to adequately measure fracture properties in the fully ductile region. Though there may be some difference in T_o values calculated with larger specimens, the results from these experiments do show a general trend of greater resistance to radiation-induced increase of T_o for the nanocluster strengthened alloy relative to the other ferritic alloys examined.

4. Conclusions

This project provided scoping information on the effects of irradiation on tensile and fracture toughness properties of two advanced dispersion strengthened ferritic alloys, 14YWT and ODS-EUROFER, which are currently being developed for structural applications in nuclear environments. Tensile results show that nanocluster strengthened 14YWT has tensile strength superior to the other ferritic alloys tested, with yield strengths of 1450 and 690 MPa measured at 26 and 600 °C, respectively. The yield strength results for ODS-EUROFER also show significant strengthening compared to non-ODS-EUROFER 97, with yield strengths of 960 and 460 MPa at 26 and 600 °C, respectively. A slight increase in yield strength (10–215 MPa, ∼1–20%) was observed for most 14YWT specimens irradiated at 580 and 670 °C, while no appreciable hardening was observed for 14YWT specimens irradiated at 300 °C. Results from specimens irradiated at 670 °C show 14YWT has good resistance to radiation-induced hardening during high-temperature irradiation for the relatively low-dose (1.5 dpa) in this study. The results suggest 14WT is also resistant to radiation-induced hardening during high-temperature irradiation, but a considerable uniform increase in yield strength of about 250 MPa (∼35% increase) was observed following relatively low-temperature (300 °C) irradiation. EUROFER 97 and ODS-EUROFER showed some radiation-induced hardening and loss of ductility, with an increase in yield strength of about 225 and 275 MPa and decrease in total elongation of about 9% and 4.5%, respectively, measured at room temperature following irradiation.

The fracture toughness results were favorable for all four ferritic alloys tested and show all alloys have low FTTT, with T_o master curve reference temperatures for the unirradiated condition ranging from −188 to −112 °C. Results from irradiated fracture toughness tests show 14YWT is resistant to radiation-induced shift in FTTT and degradation of the upper-shelf $K_{J_{Ic}}$ values, with only a 12 °C increase in T_o following irradiation and no decrease in $K_{J_{Ic}}$ values. A moderate shift in T_o (39 °C) was observed for EUROFER 97, while significant increases were exhibited by 14WT and ODS-EUROFER, at 81 and 85 °C, respectively. The low transition temperature for ductile to brittle fracture and resistance to shift in T_o observed for the 14YWT specimens tested show this alloy has significantly improved fracture toughness properties relative to previous nanocluster alloys [14]. Though the excellent fracture toughness properties observed for 14YWT, $K_{J_{Ic}}$ values near 225 MPa$\sqrt{m}$ and T_o reference temperature of −188 °C, are attrib-

uted to a refined grain structure, the coherent structure of the Y–Ti–O nanoclusters in these alloys may also reduce the number and size of microcracks that improve fracture toughness relative to conventional ODS ferritic alloys. The fracture toughness results for this nanocluster strengthened alloy are promising, and perhaps in the future dispersion strengthening may be used to increase the fracture toughness of ferritic alloys and will no longer be considered a trade-off when increasing tensile strength and creep resistance.

Acknowledgements

Special thanks are extended to Rainer Lindau of the Forschungszentrum Karlsruhe Institute for providing the advanced ODS-EUROFER alloy for this study. Research at Oak Ridge National Laboratory (ORNL) was sponsored by the US Department of Energy, Office of Fusion Energy Sciences, the US Department of Energy Office of Nuclear Energy Science and Technology, and the ORNL SHaRE Facility, which was supported in part by the Division of Scientific User Facilities, Office of Basic Energy Sciences, US Department of Energy. ORNL is managed by UT-Battelle, LLC for the US Department of Energy under Contract DE-AC05-00OR22725.

References

[1] J.J. Huet, Powder Metall. 10 (1967) 208.
[2] J.J. Huet, V. Leroy, Nucl. Technol. 24 (1974) 216.
[3] B. van der Schaaf, F. Tavassoli, C. Fazio, E. Rigal, E. Diegele, R. Lindau, G. LeMarois, Fusion Eng. Des. 69 (2003) 197.
[4] R. Lindau, A. Möslang, M. Schirra, P. Schlossmacher, M. Klimenkov, J. Nucl. Mater. 307–311 (2002) 769.
[5] R. Lindau, A. Möslang, M. Rieth, M. Klimiankou, E. Materna-Morris, A. Alamo, A.A.F. Tavassoli, C. Cayron, A.M. Lancha, P. Fernandez, N. Baluc, R. Schäublin, E. Diegele, G. Filacchioni, J.W. Rensman, B.v.d. Schaaf, E. Lucon, W. Dietz, Fusion Eng. Des. 75–79 (2005) 989.
[6] V. de Castro, T. Leguey, A. Muñoz, M.A. Monge, P. Fernández, A.M. Lancha, R. Pareja, J. Nucl. Mater. 367–370 (2007) 196.
[7] M. Klimiankou, R. Lindau, A. Möslang, J. Nucl. Mater. 367–370 (2007) 173.
[8] D.J. Larson, P.J. Maziasz, I.S. Kim, K. Miyahara, Scripta Mater. 44 (2001) 359.
[9] M.K. Miller, E.A. Kenik, K.F. Russell, L. Heatherly, D.T. Hoelzer, P.J. Maziasz, Mater. Sci. Eng. A A353 (2003) 140.
[10] M.K. Miller, D.T. Hoelzer, E.A. Kenik, K.F. Russell, Intermetallics 13 (2005) 387.
[11] R.L. Klueh, P.J. Maziasz, I.S. Kim, L. Heatherly, D.T. Hoelzer, N. Hashimoto, E.A. Kenik, K. Miyahara, J. Nucl. Mater. 307–311 (2002) 773.
[12] T. Yamamoto, G.R. Odette, P. Miao, D.T. Hoelzer, J. Bentley, N. Hashimoto, H. Tanigawa, R.J. Kurtz, J. Nucl. Mater. 367–370 (2007) 399.
[13] P. Pareige, M.K. Miller, R.E. Stoller, D.T. Hoelzer, E. Cadel, B. Radiguet, J. Nucl. Mater. 360 (2007) 136.
[14] M.A. Sokolov, D.T. Hoelzer, R.E. Stoller, D.A. McClintock, J. Nucl. Mater. 367–370 (2007) 213.
[15] D.A. McClintock, D.T. Hoelzer, M.A. Sokolov, R.K. Nanstad, J. Nucl. Mater. 386–388 (2009) 307.
[16] M.J. Alinger, G.R. Odette, D.T. Hoelzer, J. Nucl. Mater. 329–333 (2004) 382.
[17] L.L. Snead (principal developer of the SiC temperature monitor technique for HFIR rabbit capsule irradiations at Oak Ridge National Laboratory): private communication 2006.
[18] M.K. Miller, K.F. Russell, D.T. Hoelzer, J. Nucl. Mater. 351 (2006) 261.
[19] J.J. Fischer, U.S. Patent 4,075,010, Dispersion Strengthened Ferritic Alloy for use in Liquid Metal Fast Breeder Reactors, February 21, 1978.
[20] M.K. Miller, D.T. Hoelzer, E.A. Kenik, K.F. Russell, J. Nucl. Mater. 329–333 (2004) 338.
[21] M.J. Alinger, G.R. Odette, G.E. Lucas, J. Nucl. Mater. 307–311 (2002) 484.
[22] C.L. Fu, Maja Krčmar, G.S. Painter, Xing-Qiu. Chen, Phys. Rev. Lett. 99 (2007) 225502-1.